Domain 2 of Nonstructural Protein 5A (NS5A) of Hepatitis C Virus Is Natively Unfolded†

Yu Liang,‡ Hong Ye,‡ Cong Bao Kang, and Ho Sup Yoon*

Division of Structural and Computational Biology, School of Biological Sciences, Nanyang Technological University, 60 Nanyang Drive, Singapore 637511, Singapore

Received April 24, 2007; Revised Manuscript Received August 3, 2007

ABSTRACT: Nonstructural protein 5A protein (NS5A) of hepatitis C virus (HCV) plays an important role in the regulation of viral replication, interferon resistance, and apoptosis. HCV NS5A comprises three domains. Recently the structure of domain 1 has been determined, revealing a structural scaffold with a novel zinc-binding motif and a disulfide bond. At present, the structures of domains 2 and 3 remain undefined. Domain 2 of HCV NS5A (NS5A-D2) is important for functions of NS5A and involved in molecular interactions with its own NS5B and PKR, a cellular interferon-inducible serine/threonine specific protein kinase. In this study we performed structural analysis of domain 2 by multinuclear nuclear magnetic resonance (NMR) spectroscopy. The analysis of the backbone ^{1}H, ^{13}C, and ^{15}N resonances, $^{3}J_{HN\alpha}$ coupling constants ,and 3D NOE data indicates that NS5A-D2 lacks secondary structural elements and reveals characteristics of unfolded proteins. NMR relaxation parameters confirmed the lack of rigid structure in the domain. The absence of an ordered conformation and the observation of a highly dynamic behavior of NS5A-D2 may provide an underlying molecular basis on its physiological function to allow NS5A-D2 to interact with a variety of biological partners.

Hepatitis C virus (HCV[1]) is a major cause of non-A, non-B hepatitis, liver cirrhosis, and hepatocellular carcinoma (*1*). More than 170 million people have been infected with HCV worldwide (*2*). HCV is a member of the flaviviridae family, which is a linear, positive-sense, single-stranded RNA virus, approximately 9600 nucleotides long (*3*). A single open reading frame in HCV genomic RNA encodes a polyprotein precursor of 3010−3033 amino acids (*4*). Cellular signal peptidase and virally encoded proteases further process the polyprotein to at least ten mature viral proteins/enzymes, in the order of core−E1−E2−p7−NS2−NS3−NS4A−NS4B−NS5A−NS5B (*3*). The first three proteins are structural. p7, a membrane-associated protein, oligomerizes to form cation channels. NS2, NS3, NS4A, NS4B, NS5A, and NS5B are nonstructural proteins. Two of these are functionally well characterized: NS3 complexed with NS4A is a proteinase that cleaves between the nonstructural proteins (*5*). NS5B is an RNA-dependent RNA polymerase (RdRP) responsible for viral RNA synthesis (*6*, *7*).

NS5A plays critical roles in the viral replication, IFN resistance, and pathogenesis (*8*, *9*). NS5A is also involved in the apoptotic regulation (*10*), the regulation of intracellular calcium, and the elevation of reactive oxygen species in the mitochondria (*11*). The HCV protein has been predicted to contain 3 domains, domain 1 (residues 1−213), domain 2 (residues 250−342), and domain 3 (residues 356−447) (*12*). The first 30 amino acids at the N-terminus of the NS5A is the membrane anchoring domain responsible for localizing the NS5A at the endoplasmic reticulum (*13*). The N-terminal membrane anchor domain shows an in-plane amphipathic α-helix in the model membrane (*14*). A recent structural study of domain 1 (residues 36−198) revealed that it comprises a structural scaffold with a novel zinc-binding motif and a disulfide bond. The zinc-binding property is essential for HCV replication (*12*, *15*).

Domain 2 of HCV NS5A (hereafter referred as NS5A-D2) has been shown to participate in several important biological regulations: NS5A-D2 interacts with NS5B (*16*) and also contains the interferon (IFN) sensitivity-determining region, ISDR, and the protein kinase RNA-activated (PKR)-binding domain (*9*). Recently, a potential Bcl-2 homology region 2 (BH2) has also been predicted in domain 2 (*10*). Furthermore, NS5A-D2 activates PI3K by binding to the SH3 domain of the PI3K p85 regulatory subunit and results in the increased phosphorylation of Akt and the inactivation of the Akt substrates FKHR and GSK-3β (*17*, *18*).

To understand the biological role of NS5A-D2 and also provide a molecular basis of the domain when interacting with physiological partners, in this study we performed solution NMR studies of NS5A-D2. Our results indicate that NS5A-D2 is intrinsically unfolded.

MATERIALS AND METHODS

Materials. Isopropyl-thio-β-D-galactopyranoside (IPTG) was from Promega (Madison, WI). HiPrep 26/60 gel

† This study was partly supported by Singapore Cancer Syndicate Grant ZU44.

* Author to whom correspondence should be addressed. E-mail: hsyoon@ntu.edu.sg. Phone: +65 6316-2846. Fax: +65 6791-3856.

‡ These authors contributed equally to this work.

[1] Abbreviations: HCV, hepatitis C virus; NS5A, nonstructural protein 5A; NMR, nuclear magnetic resonance; CD, circular dichroism; IFN, interferon; BH, Bcl-2 homology region; IPTG, isopropyl-thio-β-D-galactopyranoside; PMSF, phenylmethylsulfonyl fluoride; CSI, chemical shift index; TFE, 2,2,2-trifluoroethanol.

10.1021/bi700776e CCC: $37.00
Published on Web 09/19/2007

Sephacryl S-200 gel filtration column was from Amersham Biosciences (Buckinghamashire, U.K.). ^{15}N-NH_4Cl and ^{13}C-glucose were from Cambridge Isotope Laboratories (MA). NS5B peptides for NMR titration assay were obtained from GL Biochem. Ltd. (Shanghai, China). All the other chemicals were obtained from Sigma (St. Louis, MO).

Expression and Purification of ^{15}N- and ^{15}N/^{13}C-Labeled NS5A-D2 (Amino Acids 240−*335).* Plasmids pET-Ub-NS5A-D2-His were co-transformed with pCG1 (a gift from Dr. Craig Cameron), which encodes the yeast ubiquitin C-terminal protease, into *Escherichia coli* BL21 (DE3) cells in the presence of 30 μg/mL kanamycin and 25 μg/mL chloramphenicol. A preculture (2 mL) was grown overnight in 25 mL of M9 medium containing ^{15}N-NH_4Cl or both ^{15}N-NH_4Cl/^{13}C-glucose, supplemented with 30 μg/mL kanamycin, and 25 μg/mL chloramphenicol at 37 °C. The overnight culture was diluted by 100-fold into 1 L of M9 medium containing ^{15}N-NH_4Cl or ^{15}N-NH_4Cl/^{13}C-glucose with 30 μg/mL kanamycin and 25 μg/mL chloramphenicol. Cells were grown at 37 °C to the absorbance of 0.8−1.0 at 600 nm and induced with 0.5 mM isopropyl-β-D-thiogalactopyranoside (IPTG) for an additional 4 h at 20 °C. Approximately 5 g of cell pellet was resuspended in 30 mL of lysis buffer (100 mM Tris-Cl, pH 7.0, 200 mM NaCl, 20 mM imidazole, 1 mM phenylmethylsulfonyl fluoride (PMSF), 5 mM 2-mercaptoethanol), and lysed by sonication for 20 min in ice. The disrupted cell lysate was centrifuged at 20000*g* for 30 min. The supernatant was loaded onto 1 mL of Ni^{2+}-NTA agarose column (Qiagen, Hiden, Germany) pre-equilibrated with the lysis buffer and washed with 10 mL of the lysis buffer, followed by 20 mL of washing buffer (100 mM Tris-Cl, pH 7.0, 1 M NaCl, 50 mM imidazole, 1 mM PMSF, 5 mM 2- mercaptoethanol), and the protein was eluted by the elution buffer (100 mM Tris-Cl, pH 6.4, 200 mM NaCl, 500 mM imidazole, 1 mM PMSF, 5 mM 2-mercaptoethanol). The eluted NS5A-D2 was further purified by high-resolution Sephacryl S-200 gel filtration column (Amersham Biosciences, Buckinghamashire, U.K.). The purified protein samples were analyzed on 15% SDS−PAGE gel, and protein concentration was determined by a protein assay kit from Bio-Rad Laboratories (Hercules, CA). Proteins were stored at 4 °C before use. For biochemical studies, NS5A-D2 was expressed in *E. coli* BL21(DE3) cells grown on a NZCYM medium and purified using Ni^{2+}-NTA affinity followed by Sephacryl S-200 gel filtration column chromatography.

Circular Dichroism (CD) Spectroscopy. The CD spectrum of the NS5A-D2 (100 μM) was recorded in 20 mM sodium phosphate, pH 6.5, 50 mM sodium chloride buffer on a Chirascan (Applied Photophysics Limited, Surrey, U.K.). The above-mentioned buffer was used as a blank, and the spectrum with 4 scans was recorded from 180 to 280 nm at 25 °C. 2,2,2-Trifluoroethanol (TFE)-induced structural change was examined using the above sample in the presence of various concentrations of TFE.

NMR Sample Preparation. The uniformly ^{15}N- and ^{15}N/^{13}C-labeled NS5A-D2 samples for NMR experiments were used at a final concentration of 0.6 mM in 20 mM $NaPO_4$, pH 6.5, 50 mM NaCl, 1 mM DTT, 0.01% NaN_3, and 90% H_2O/10% D_2O.

NMR Data Collection and Assignment. All backbone assignment experiments for the ^{15}N/^{13}C-labeled NS5A-D2 (102 residues) were done at 298 K on a Bruker AV700 spectrometer equipped with a cryoprobe accessory. Backbone ^{1}H, ^{15}N, ^{13}C resonances were assigned using data from 2D ^{1}H−^{15}N HSQC, 3D HNCA, HN(CO)CA, HNCO, HNCACB, CBCA(CO)NH, and HNHA spectra (*19*). The side chain ^{1}H and ^{13}C resonances were obtained from 3D HCC(CO)NH-TOCSY, HCCH-TOCSY, and ^{1}H−^{15}N NOESY-HSQC. To investigate conformation of NS5A-D2 at low temperature, backbone/side chain experiments and 3D ^{1}H−^{15}N NOESY-HSQC were also collected at 278 K. All spectra were processed by Topspin version 1.3 (Bruker) and analyzed using Felix (Accelrys) and NMRView (*20*).

NMR Relaxation Measurements. Backbone ^{15}N relaxation measurements were carried out at 700 MHz as described previously (*21*, *22*). Twelve and ten *T* delays were used for T_1 (21, 54, 108, 162, 270, 432, 648, 864, 1188, 1512, 1944, 2268 ms) and T_2 (14.4, 28.8, 43.2, 57.6, 72, 100.8, 129.6, 158.4, 187.2, 230.4 ms), respectively. The interscan delay was 1.5 s for the ^{15}N T_1 and T_2 experiments. The rates were fit with the program Felix (Accelrys) to a two-parameter single-exponential decay. Heteronuclear NOE experiments were performed using a 2 s interscan delay followed by either 3 s of proton saturation using a series of 120° ^{1}H pulses or an additional 3 s delay at 298 and 278 K respectively.

NMR Titration To Study NS5A-D2 and NS5B MK-17 Peptide Interaction. Two peptides derived from NS5B (residues 139−155, MAKNEVFCVQPEKGGRK, referred as to MK-17; residues 365−388, SCSSNVSVAHDGAGKRVYYLTRDP, hereafter referred as to SP-24) were synthesized (GL Biochem. Ltd., Shanghai, China). Uniformly ^{15}N-labeled NS5A-D2 with a concentration of 0.2 mM was prepared in a buffer containing 20 mM $NaPO_4$, pH 6.5, 50 mM NaCl, 0.1% NaN_3, 1 mM DTT. ^{1}H−^{15}N HSQC spectra were collected at 298 K with varying molar ratio between ^{15}N-labeled protein and the peptides on a Bruker 600 MHz with a cryoprobe.

RESULTS

NMR Resonance Assignments. Assignments of ^{1}H, ^{13}C, and ^{15}N resonances have been made by using three-dimensional heteronuclear NMR spectroscopy. We have assigned $^{13}C^{\alpha}$ resonances for 94 residues and $^{13}C^{\beta}$ resonances for 92 residues (two glycines with no $^{13}C^{\beta}$) out of 102 residues in NS5A-D2, respectively. The unassigned residues are K1, P84, and the C-terminal His_6-tag. As shown in Figure 1, backbone residues out of 94 non-proline residues in NS5A-D2 were resolved, except for K1, A2, and the C-terminal His_6-tag. The chemical shifts of the backbone amide proton resonances are clustered in a narrow 1.3 ppm window from 7.2 to 8.5 ppm, and the dispersion of the ^{15}N chemical shifts is narrowed in 19.2 ppm, as typical signs of an unfolded protein (*23*). The backbone resonances are clustered in three regions in the spectra. A bulk of the ^{15}N chemical shifts for the backbone amides are clustered between 116.4 and 127.4 ppm. The ^{15}N chemical shifts for Gly residues are resonated between 108.1 and 109.3 ppm. The ^{15}N chemical shifts for Thr/Ser residues are mostly clustered between 114.1 and 116.5 ppm, consistent with the characteristic ^{15}N chemical shifts of amino acid residues in unfolded conformations (*24*). Excluding K1 and the C-terminal His_6-tag residues, the assignments of the side chains are about 80%

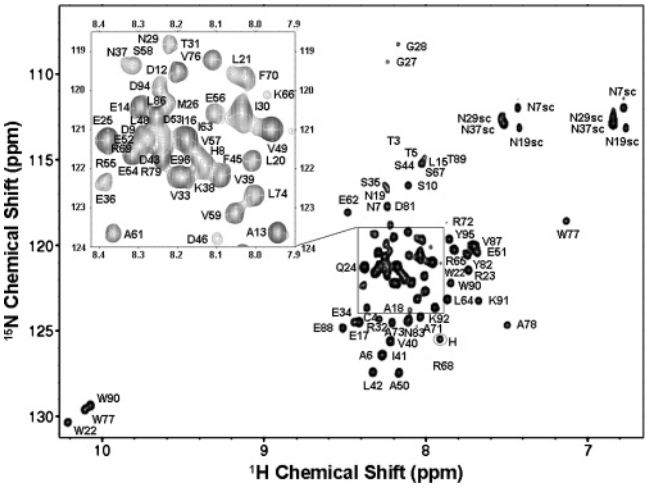

FIGURE 1: 2D ^{1}H−^{15}N HSQC spectrum of NS5A-D2. The uniformly ^{15}N-labeled NS5A-D2 was prepared at a final concentration of 0.6 mM in 20 mM $NaPO_4$, pH 6.5, 50 mM NaCl, 1 mM DTT, 0.01% NaN_3, and 90% H_2O/10% D_2O, and the spectrum was recorded at 298 K on a 700 MHz instrument equipped with cryoprobes. Backbone amide proton resonances are narrowly dispersed over the range of 7.2 to 8.5 ppm. The rectangle region is expanded to allow labeling of the crowded central region of the spectrum. Backbone resonance assignments of 86 out of the 94 non-proline residues of NS5A-D2 are shown. Side chain Asn $-NH_2$ resonances and side chain Trp −NH resonances are also shown. The dashed ellipse outlines one of the last five histidines in His_6-tag based on backbone and side chain assignments.

complete. The cross peaks for the side chain amides of the carboxyamide groups in four Asn (between 6.7 and 7.5 ppm for ^{1}H, between 111.9 and 113.1 ppm for ^{15}N, respectively) and the NH of the rings of three Trp (between 10 and 10.2 ppm for ^{1}H, between 129.3 and 130.3 ppm for ^{15}N, respectively) are also visible in the 2D ^{1}H−^{15}N HSQC spectrum. The chemical shifts of the $-NH_2$ side chain protons of the four Asn resonate at the chemical shifts indicative of short unstructured peptides (*25*). This feature is not usually displayed in the spectra of native folded proteins because longer range specific contacts always induce the chemical shift perturbations (*26*).

Secondary Chemical Shifts of NS5A-D2. As a sensitive indicator of conformation, NMR backbone chemical shift assignment allows secondary structure analysis through comparison with the random coil values (termed as secondary chemical shift, $\Delta\delta$) corrected for local sequence effects (*27*). For $^{13}C^{\alpha}$ and ^{13}CO, positive secondary chemical shifts compared with those of random coils indicate a preference for helical conformations whereas negative values indicate a propensity toward extended conformations in β-sheet region. The trend is reversed for $^{1}H^{\alpha}$ and $^{13}C^{\beta}$, with negative values indicating helical conformations and positive values indicating β-sheet (*28*−*30*). As shown in Figure 2a, multinuclear (CA, CB, HA, and CO) chemical shift indexing, consensus CSI (*30*) values are zeros, suggesting that NS5A-D2 largely exists in a random coil conformation. Although the CSI values of HA suggest an indication of possible α-helix characters in some regions of NS5A-D2, similar to the previous prediction (*12*), CSI values of CA, CB, and CO do not support presence for consistent helical structures.

Analysis of Coupling Constant and NOE Data for NS5A-D2. To evaluate if there are any folded structures present, we measured $^{3}J_{HN\alpha}$ coupling constants from a 3D HNHA experiment (*31*) and also analyzed 3D ^{1}H−^{15}N NOESY-HSQC (*32*). As shown in Figure 2b, the majority of $^{3}J_{HN\alpha}$ coupling constants ranged from 5 to 8 with an average value of 6.607 ± 1.157, giving no evidence of the presence of any α-helix, β-sheet, or β-turns. A summary of the NOEs involving the HN, C_α, and C_β protons is shown in Figure 2c. Sequential NH (*i*)−NH (i + 1) NOEs and C_αH (*i*)−NH (i + 1) NOEs are observed for several regions. C_βH (*i*)−NH (i+1) NOEs are also seen for some residues. Only two weak C_αH (*i*)−NH (i + 2) NOEs are observed (between E52 and E54; R72 and L74). Overall, the NOE data of NS5A-D2 provided no evidence for any significant nonsequential NOEs, which is an indication for the presence of a folded conformation.

Backbone Dynamics of NS5A-D2. The backbone dynamics of the uniformly ^{15}N-labeled NS5A-D2 were studied by 2D ^{15}N-relaxation measurements at 298 K. The steady-state heteronuclear ^{1}H−^{15}N NOE for the backbone amide of NS5A-D2 exhibited a relatively featureless and flattened variation with the amino acid sequences (Figure 3a), as seen in unfolded proteins (*33*). The mean value of heteronuclear ^{1}H−^{15}N NOEs was 0.24 at 700 MHz, while those of folded proteins with similar lengths of polypeptide chain were higher than 0.5 (*34*, *35*). The lower NOE values for NS5A-D2 reflect more unrestricted dynamics on the nanosecond to picosecond time scales than those for the folded proteins. The region from I41 to F70 shows slightly higher NOE values than the rest, suggesting the presence of relatively rigid structure. A significant deviation from the average values was observed for R72.

The resulting ^{15}N T_1 and T_2 data are summarized in Figure 3b and 3c. The T_1 values appear to be uniform, with a mean value of 0.64 s. The mean T_2 value is 0.18 s. In folded proteins similar in size to NS5A-D2, the average T_2 values are on the order of 0.12 s (*35*). In general, high T_2 values indicate unrestricted fast dynamics, whereas low values suggest restricted fast dynamics and possible slow conformational exchange (*36*). The high T_2 values measured for NS5A-D2 indicate large amplitude motions on the nanosecond to picosecond time scale, which is characteristic of a random coil conformation.

Effect of Chemical Denaturants. To analyze the stability of proteins, the two-state model of protein unfolding in chemical denaturants is commonly used. In this model, there are a native state and an unfolded state. The energetics of this transition depends on the difference in the structure between the two states (*37*). To detect whether there is any structural difference between the native NS5A-D2 and the chemical denaturant-treated NS5A-D2, we performed the measurements of 2D ^{1}H−^{15}N HSQC for these two states. Figure 4 shows the effects of 8 M urea on the ^{1}H−^{15}N HSQC correlation spectrum of NS5A-D2. The global patterns of the two spectra are similar, with the features of the unfolded proteins including the narrow bulk window, the three typical separated regions of the residue random coil positions (Gly, Thr/Ser, and other backbone amides), and the $-NH_2$ side chain protons of Asn resonating at the chemical shifts found for short unstructured peptides (*24*−*26*). The results suggest that the native state NS5A-D2 by and large resembles the chemical-induced unfolded state. However, upon comparing the 2D ^{1}H−^{15}N HSQC correlation spectra of two states, we noticed that there are a few residues undergoing chemical

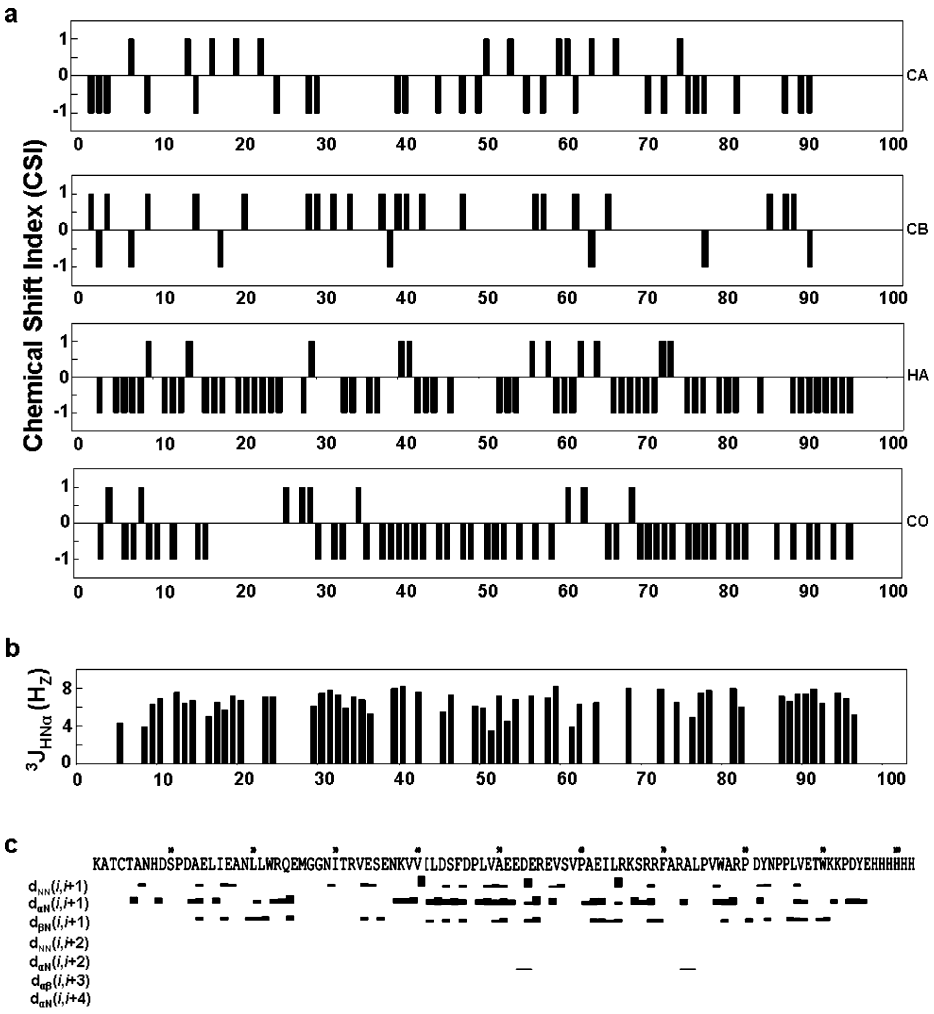

FIGURE 2: Summary of the NMR parameters defining the conformational characteristics of NS5A-D2 at 298 K. (a) Chemical shift index plots of CA, CB, HA, and CO. Chemical shift values were taken from CSI v2.0 (*63*). The consensus CSI values are zeros, indicating a random coil conformation. (b) $^3J_{HN\alpha}$ coupling constants measured for NS5A-D2 at 298 K. (c) Variations for NOE intensities for the NS5A-D2 observed in the 3D NOESY-HSQC spectrum recorded with a mixing time of 100 ms.

shift perturbations, suggesting the possible presence of transient secondary structures between the two states.

Effect of TFE. The typical CD spectrum of α-helices is characterized by minima near 208 and 222 nm, the *β*-sheet structures yield a minimum at 215 nm, and random coil structures are characterized by a negative peak near 200 nm (*38*). As shown in Figure 5a, the CD spectrum of NS5A-D2 without TFE exhibits a minimum near 201 nm, with a slight negative ellipticity at about 222 nm, suggesting that it is mainly unfolded. While at lower TFE concentration (10% and 20%) the protein appeared highly aggregated (data not shown), TFE-induced cooperative transition to α-helix formation of NS5A-D2, which is characterized by minimum near 208 and 222 nm, was observed at 40% TFE and even more obviously at 60% TFE. We also recorded the $^1H-^{15}N$ HSQC spectrum of the ^{15}N-labeled NS5A-D2 upon the addition of 60% TFE (Figure 5b), showing broadening of the amide proton line widths and significant chemical shift perturbations. The chemical shift perturbations in ^1H and ^{15}N in the presence of 60% TFE appears to favor a transition toward α-helix (*39*).

Effect of Low Temperature. To investigate any potential conformation change of NS5A-D2 at low temperature, backbone and side chain assignment data were collected at 278 K. $^3J_{HN\alpha}$ coupling constants, 3D NOEs, and dynamic heteronuclear $^1H-^{15}N$ NOE were also measured. Compared to the 2D $^1H-^{15}N$ HSQC spectrum at 298 K, the spectrum at 278 K still shows a lack of chemical shift dispersion but with overall upfield shift for ^1H (data not shown). The CSI values of HA for 278 K show largely a propensity to α-helix character, but the consensus CSI values are zeros, indicating that NS5A-D2 is still predominantly unstructured at low temperature.

As shown in Figure 6a, at 278 K, the average value of $^3J_{HN\alpha}$ coupling constants was 6.1654 ± 1.028, a little lower than that of 298 K. The summary of the NOEs involving the HN, C_α, and C_β protons at the temperature is also shown in Figure 6b. At lower temperature more sequential NH (*i*)−NH ($i + 1$) NOEs, C_αH (*i*)−NH ($i + 1$) NOEs, and C_βH (*i*)−NH ($i + 1$) NOEs were observed compared to those of 298 K, especially for the region from T3 to V40. In addition, more NH (*i*)−NH ($i + 2$) and C_αH (*i*)−NH ($i + 2$) NOEs were seen at lower temperature.

As shown in Figure 6c, the mean value of heteronuclear $^1H-^{15}N$ NOEs is 0.3866 and is a little higher than that of 298 K, suggesting that NS5A-D2 is more stable at low

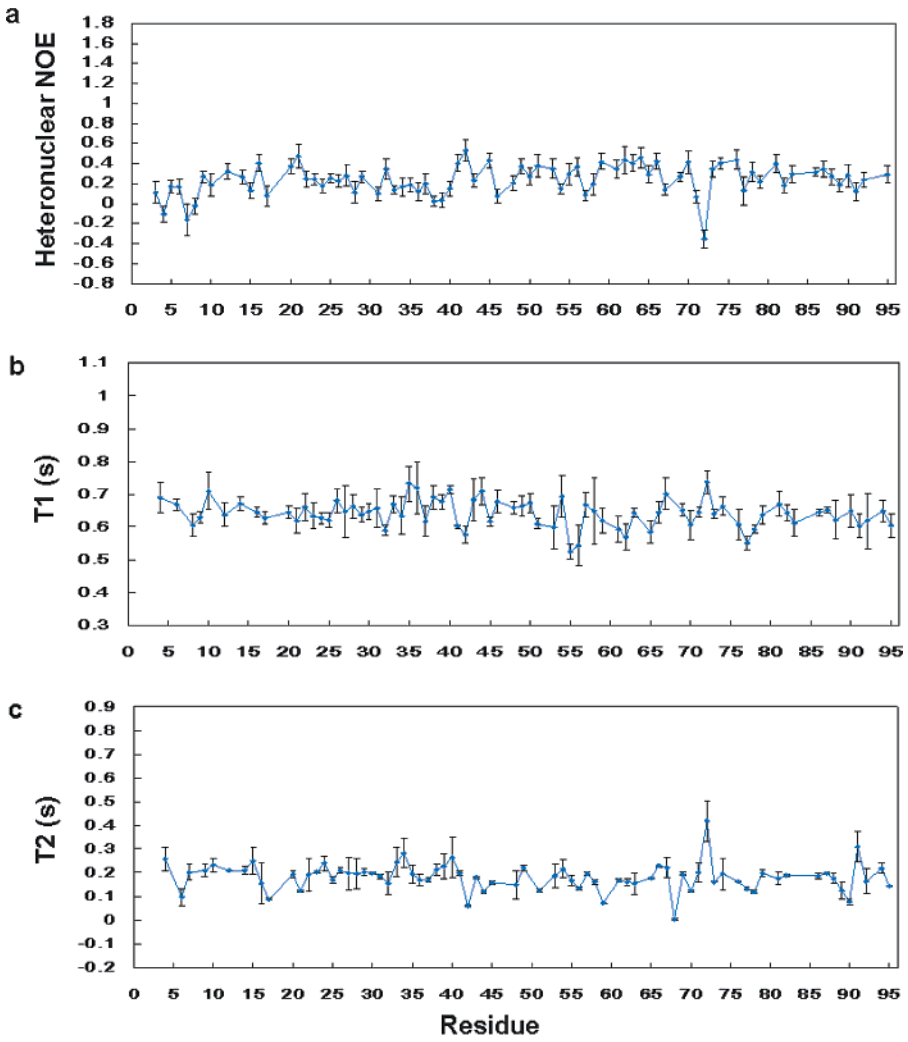

FIGURE 3: Relaxation measurements of NS5A-D2. (a) Steady-state heteronuclear $^{1}H-^{15}N$ NOE for the backbone amide of NS5A-D2 at 298 K. (b) Longitudinal relaxation, T_1. (c) Transverse relaxation, T_2. The schematic plots illustrate dynamics of the backbone.

temperature, especially the region from T3 to V40. However, the spectrum still appears relatively flattened and featureless. The mean value is lower than that of the folded protein with similar size (*34*, *35*), indicating NS5A-D2 is in unfolded conformation. The result is consistent with that of $^{3}J_{HN\alpha}$ coupling constants and 3D NOEs.

Taken together, there is a trend for NS5A-D2 to be helical and the protein appears to be less flexible at low temperature. However, the protein is still not in well-folded conformation.

Binding of NS5A-D2 to HCV NS5B. NS5B has a GDD motif common to all RNA polymerases of RNA viruses and has been shown to possess RNA-dependent RNA polymerase (RdRP) activity (*6*, *7*). It has been elucidated that HCV NS5A directly interacts with HCV NS5B as a component of HCV replicase complex and NS5A-D2 contains the binding sites for NS5B protein (*16*). To determine the binding ability of NS5A-D2 to HCV NS5B, we analyzed the molecular interaction by NMR spectroscopy. Based upon the previously reported sequences of NS5B essential for binding to NS5A (*16*), the MK-17 peptide, which contains residues 139−155 of NS5B, and SP-24 peptide which contains residues 365−388 of NS5B, were designed for NMR studies. Our NMR results showed that perturbations in the chemical shifts were observed in $^{1}H-^{15}N$ HSQC spectrum of ^{15}N-labeled NS5A-D2 in the presence of 5 mM of the MK-17 peptide (Figure 7a), whereas the titration with the peptide SP-24 caused a heavy precipitate upon its addition (data not shown). While many residues of NS5A-D2 experience chemical shift perturbations upon the addition of the MK-17 peptide, however, the residues most affected with an increasing concentration of the peptide MK-17 less than 2 mM appear to be localized to two regions: L48−V57 and L86−E96. As shown in Figure 7b, Y95 showed the most obvious shift at this stage. Interestingly, as the ligand concentration gradually increased over 2 mM, we have observed that residues from other region began to show apparent chemical shift perturbation; for instance, amino acid R68 exhibited noticeable chemical shift perturbation in the presence of an increasing amount of the peptide ranging from 2 mM to 4 mM (Figure 7b). These data suggest that NS5A-D2 undergoes conformational changes upon binding the MK-17 peptide. Consistent with the previous report (*16*), the purified NS5A-D2, despite its disordered state, still maintains the binding capacity to its biological ligand.

DISCUSSION

Domain 2 of HCV NS5A contributes to the multiple functions of NS5A in viral replication or other regulations. Currently, the precise function and structure of this domain is still unclear. In this study, we examined structural features

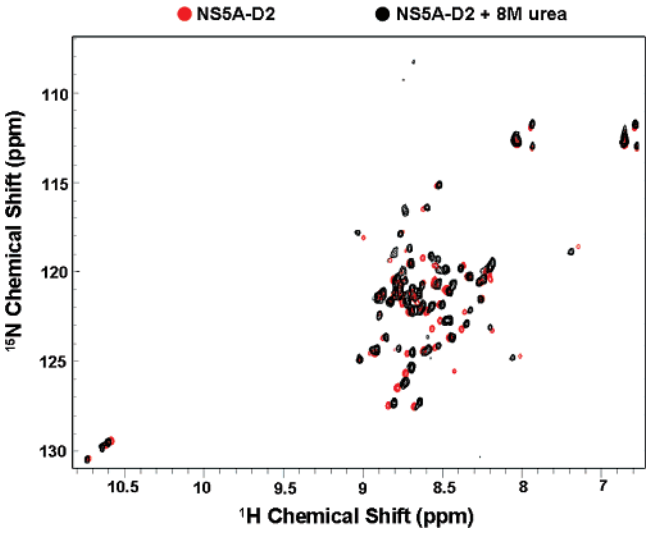

FIGURE 4: Effect of chemical denaturants on the structure of NS5A-D2. Two-dimensional ^{1}H−^{15}N HSQC spectra of NS5A-D2 were recorded in the absence and presence of 8 M urea. Concentrations of the uniformly ^{15}N-labeled samples for the NMR study were 0.2 mM. The spectra were collected at pH 6.5 and 298 K. The ^{1}H−^{15}N HSQC spectrum of NS5A-D2 (red) was overlaid with the 8 M urea-treated spectrum (black).

of NS5A-D2 (amino acids 240−335) of HCV, which covers the PKR/NS5B binding site. The pattern of the 2D ^{1}H−^{15}N HSQC spectrum of the free NS5A-D2 is similar to those found in unfolded proteins (*23*−*25*). The analysis of the backbone assignments by CSI (*30*) suggests that NS5A-D2 lacks ordered secondary structures. $^{3}J_{HN\alpha}$ coupling constants and 3D NOE data for NS5A-D2 do not appear to provide supporting evidence of any ordered secondary structural elements. All the resulting T_1, T_2, and heteronuclear ^{1}H−^{15}N NOE values of NS5A-D2 indicate unrestricted dynamics on the nanosecond to picosecond time scales. The measurements of both static and dynamic multinuclear NMR parameters indicate that the free NS5A-D2 exists predominately in a random coil conformation.

An earlier study revealed that a half of the protein sequences in the Swiss Protein Database contained segments of low complexity that correspond to nonglobular regions (*40*). The mean hydrophobicity *versus* mean net charge values suggest that the NS5A-D2 sequence has an overall low hydrophobicity and a high net positive charge, similar to those of natively unfolded proteins (Figure 8). Generally, the formations of a hydrophobic core and rigid secondary structure are not favored with the low content of hydrophobic amino acid residues (*41*, *42*). The analysis of the charge distribution of the residues in NS5A shows three acidic domains located in the region from residues 220 to 300 (*43*), mainly part of NS5A-D2. Low content of hydrophobic amino acid residues surrounded by numerous acidic residues can also result in an extended conformation because of the electrostatic repulsion (*44*).

Compared to folded proteins, one advantage that unfolded proteins might have is that they provide a much larger surface area, which would allow multiple molecular interactions (*45*). Unstructured proteins are inherently flexible. Unfolded proteins may have advantages to respond to environmental factors, and their local and global structures can be easily adapted in cellular environments. The intrinsic structural flexibility of the unstructured proteins could permit a single

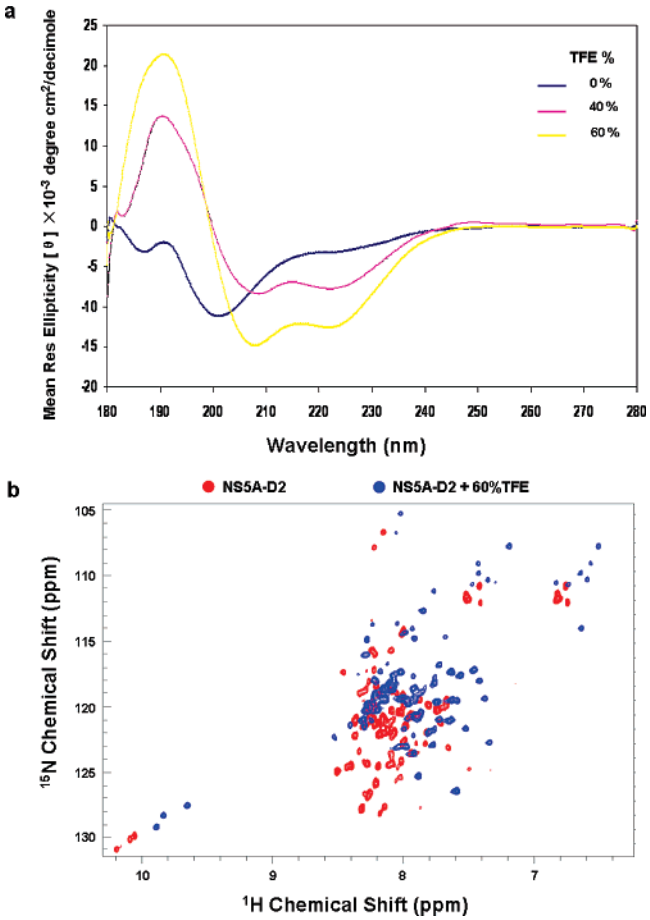

FIGURE 5: TFE-dependent conformational transition of NS5A-D2 measured by CD and 2D ^{1}H−^{15}N HSQC at 25 °C. (a) CD spectra of 100 μM NS5A-D2 (blue line), NS5A-D2 in the presence of 40% TFE (pink line) and in the presence of 60% TFE (yellow line) at pH 6.5. (b) Chemical shift perturbations of the ^{15}N-labeled NS5A-D2 was monitored on a 2D ^{1}H−^{15}N HSQC upon the addition of 60% TFE. The spectrum of NS5A-D2 in aqueous solution is shown in red while the spectrum of NS5A-D2 in 60% TFE is shown in blue.

protein to recognize a large number of biological targets without sacrificing specificity (*46*). The most common types of intrinsically unstructured protein are DNA-binding domains of transcription factors (*47*), transcriptional activation domains of transcription regulators (*48*−*50*) and kinases (*51*). The unfolded structure of NS5A-D2 determined by our current NMR studies possibly provides a molecular basis to its multiple functions such as binding with different biological partners of NS5A including NS5B, PKR, TRAF2, and Grb2, participating in the activation of transcription, IRES suppression, and anti-apoptosis.

Compared to water, TFE is a slightly stronger proton donor, but a much weaker proton acceptor (*52*). In an aqueous solution TFE can strengthen the intramolecular hydrogen bonds to stabilize the α-helical conformation (*53*). The effects of TFE have also been found to be sequence-dependent (*54*) and appear to be correlated with the propensity of α-helix formation (*55*). Our results indicate that in the presence of 40% or 60% TFE, NS5A-D2 demonstrated a cooperative transition from random coil to α-helix conformation. This indicates that NS5A-D2 has a possible transition structure with propensity to form helix.

According to the data of $^{3}J_{HN\alpha}$ coupling constants and 3D NOEs of NS5A-D2 at 278 K, some helical trend was

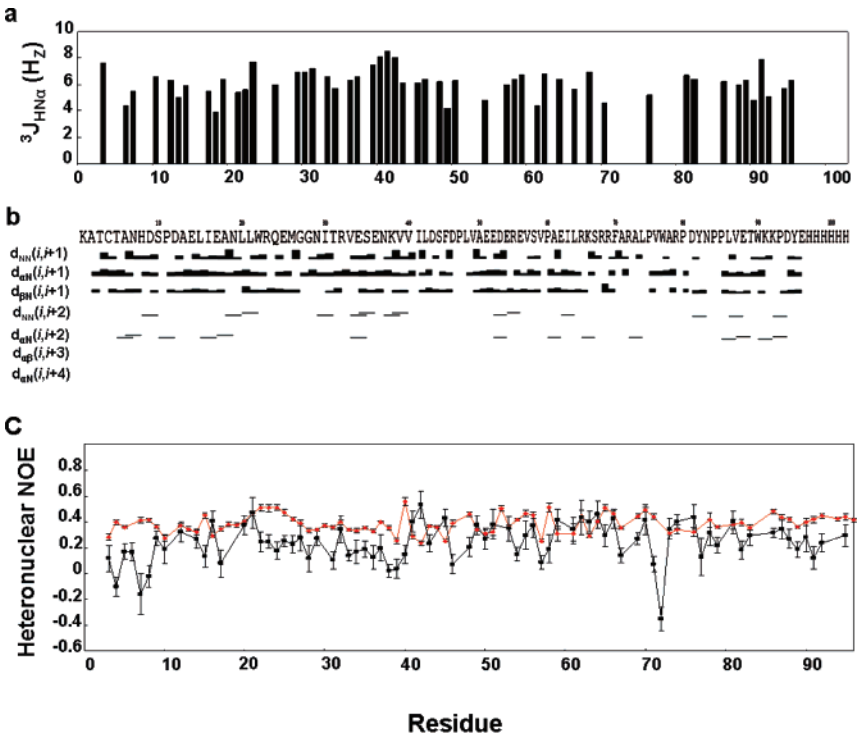

FIGURE 6: Summary of the NMR parameters defining the conformational characters of NS5A-D2 at 278 K. (a) $^3J_{HN\alpha}$ coupling constants measured for NS5A-D2 at 278 K. (b) Variations for NOE intensities for the NS5A-D2 observed in the 3D NOESY-HSQC spectrum recorded with a mixing time of 100 ms at 278 K. (c) Comparison of steady-state heteronuclear $^1H-^{15}N$ NOE for the backbone amide of NS5A-D2 at 278 K (in red) to that of 298 K (in black).

observed. Additionally, the mean steady-state $^1H-^{15}N$ heteronuclear NOE value is a little higher than that of 298 K. Even though it still remains unfolded conformation, the NMR data at 278 K suggest that NS5A-D2 is more stable at low temperature, indicating the presence of environment-sensitive conformation of NS5A-D2.

Natively unfolded proteins undergo partial or full folding processes upon binding to biological partners (*56*, *57*). In unfolded proteins, the regions with residual structures are critical for forming the initial site of interaction with binding partners (*57*). In our NMR titration study of NS5A-D2 with the MK-17 peptide, noticeable chemical shift perturbations were observed, suggesting the molecular interaction between these two molecules (Figure 7). Previously we have shown that NS5A-D2 of HCV also binds another biological partner PKR (*58*). Taken together, our results suggest that NS5A-D2 is natively in an unfolded state but can interact with its biological partners.

During our studies using NMR, we observed that when the amount of peptide is lower than 2 mM (20-fold excess compared to that of NS5A-D2), although some perturbations in the chemical shifts were detected, no great changes happened to the overall HSQC spectrum (data not shown). At the point when the peptide concentration reached 2 mM, a heavy precipitation appeared. Interestingly, as we increased the MK-17 peptide concentration from 2 mM to 5 mM, the precipitation gradually disappeared and the solution finally became transparent again at the point of 5 mM peptide concentration (50-fold excess of the NS5A-D2). Both the line widths and dispersion of the HSQC spectrum of NS5A-D2 with 5 mM MK-17 were affected, similar to the spectrum of NS5A-D2 in the presence of 60% TFE to a certain degree. This indicates that the interaction between domain 2 and the

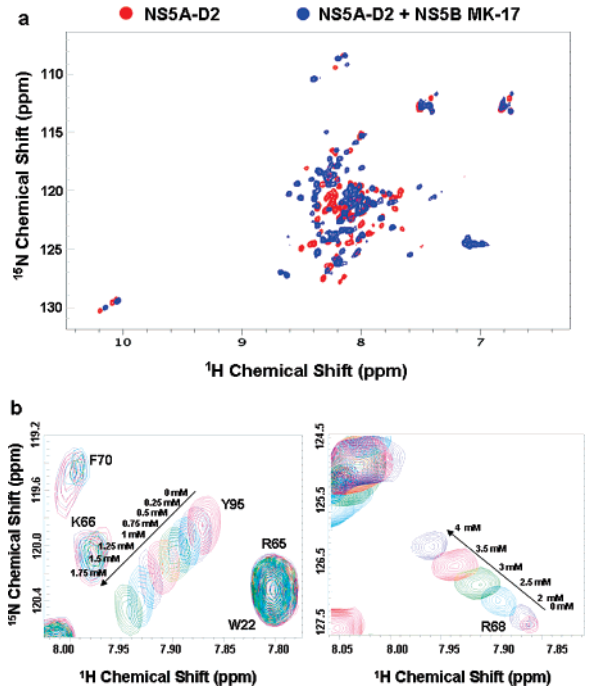

FIGURE 7: NS5A-D2 interacts with NS5B MK-17 peptide. (a) Chemical shift perturbations of the ^{15}N-labeled NS5A-D2 were monitored on a 2D $^1H-^{15}N$ HSQC upon the addition of the unlabeled NS5B MK-17 peptide. The spectrum of free NS5A-D2 is shown in red while the spectrum of NS5A-D2 with the addition of NS5B MK-17 peptide is shown in blue. Concentrations of ^{15}N-labeled NS5A-D2 and NS5B MK-17 peptide were 0.1 mM and 5 mM, respectively. (b) Section of the 2D $^1H-^{15}N$ HSQC of ^{15}N-labeled NS5A-D2 titrated with unlabeled NS5B MK-17 peptide. Amino acid Y95 chemical shifts were changed upon the addition of increasing amount of MK-17 from 0 to 1.75 mM as displayed. Amino acid R68 chemical shifts were changed upon the addition of increasing amount of MK-17 from 0 to 4 mM.

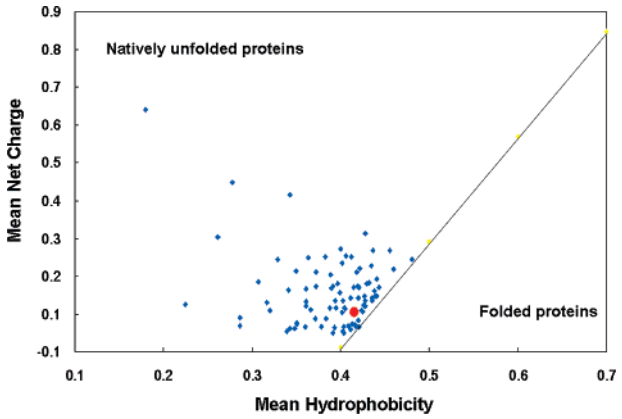

FIGURE 8: Charge-hydrophobicity phase space plotted for NS5A-D2. The diagram plots the correlation between the mean hydrophobicity $\langle H \rangle$ and the mean net charge $\langle R \rangle$ for a set of 90 natively unfolded proteins as indicated in diamond as previously described (*44*), and NS5A-D2 is shown in red circle. The solid black line represents the boundary between natively unfolded and folded proteins (*44*): $\langle R \rangle = 2.785 \langle H \rangle - 1.151$.

MK-17 peptide results in conformation changes. The accumulations of folding intermediates tending to aggregate are commonly observed during the course of protein folding (*59*−*61*). It might be possible that the MK-17 peptide at 2 mM induces conformational change of NS5A-D2 resulting in a folding intermediate that might cause a heavy aggregation. From folding energy landscape, without sufficient energetic interactions natively unfolded proteins appear to have no ability compensate conformational entropy to form a globular state. Therefore, interactions with their ligands or oligomerization might contribute to achieving structural stability of the unfolded proteins (*62*). This principle could explain the phenomenon that was seen with the increasing of the peptide from 2 mM to 5 mM, showing that the aggregation of NS5A-D2 gradually disappeared and finally reached a more stable conformation. The requirement of the higher concentration of the MK-17 peptide might be due to the faster dissociation of the peptide from the binding site on NS5A-D2. Alternatively, the ligand concentration-dependent conformational changes might involve a potential cooperativity in the structural transition of the NS5A-D2.

In summary, our results suggest that NS5A-D2 exists intrinsically unfolded, but it still maintains in its functional state. The NMR parameters reflecting backbone dynamics of NS5A-D2, the difference in 2D $^{1}H-^{15}N$ HSQC spectrum between the native NS5A-D2 and the chemical denaturant-induced NS5A-D2, and the more stable status of NS5A-D2 at low temperature are indicative of existence of a potential transition between ordered and disordered structures. The molecular interaction between the NS5A-D2 and the MK-17 peptide appears to induce conformation change under the condition used in this study. It remains to be further explored that the molecular interaction of NS5A-D2 with physiological ligands such as full-length NS5B, PKR, or other partners could induce a global conformational change of the intrinsically disordered NS5A-D2 to a more stable folded state.

ACKNOWLEDGMENT

We thank Dr. Craig Cameron for providing pCG, Dr. Ding Xiang Liu for HCV 1a genomic DNA, and Dr. Salil Bose for valuable comments on the manuscript.

REFERENCES

1. Choo, Q. L., Kuo, G., Weiner, A. J., Overby, L. R., Bradley, D. W., and Houghton, M. (1989) Isolation of a cDNA clone derived from a blood-borne non-A, non-B viral hepatitis genome, *Science 244*, 359−362.
2. Lavanchy, D. (1999) Hepatitis C: public health strategies, *J. Hepatol. 31* (Suppl. 1), 146−151.
3. Miller, R. H., and Purcell, R. H. (1990) Hepatitis C virus shares amino acid sequence similarity with pestiviruses and flaviviruses as well as members of two plant virus supergroups, *Proc. Natl. Acad. Sci. U.S.A. 87*, 2057−2061.
4. Saito, I., and Miyamura, T. (1990) [Hepatitis C virus], *Protein, Nucleic Acid Enzyme 35*, 2117−2127.
5. Failla, C., Tomei, L., and De Francesco, R. (1994) Both NS3 and NS4A are required for proteolytic processing of hepatitis C virus nonstructural proteins, *J. Virol. 68*, 3753−3760.
6. Behrens, S. E., Tomei, L., and De Francesco, R. (1996) Identification and properties of the RNA-dependent RNA polymerase of hepatitis C virus, EMBO *J. 15*, 12−22.
7. Lohmann, V., Korner, F., Herian, U., and Bartenschlager, R. (1997) Biochemical properties of hepatitis C virus NS5B RNA-dependent RNA polymerase and identification of amino acid sequence motifs essential for enzymatic activity, *J. Virol. 71*, 8416−8428.
8. Blight, K. J., Kolykhalov, A. A., and Rice, C. M. (2000) Efficient initiation of HCV RNA replication in cell culture, *Science 290*, 1972−1974.
9. Gale, M. J., Korth, M. J., Tang, N. M., Tan, S. L., Hopkins, D. A., Dever, T. E., Polyak, S. J., Gretch, D. R., and Katze, M. G. Jr. (1997) Evidence that hepatitis C virus resistance to interferon is mediated through repression of the PKR protein kinase by the nonstructural 5A protein, *Virology 230*, 217−227.
10. Chung, Y. L., Sheu, M. L., and Yen, S. H. (2003) Hepatitis C virus NS5A as a potential viral Bcl-2 homologue interacts with Bax and inhibits apoptosis in hepatocellular carcinoma, *Int. J. Cancer 107*, 65−73.
11. Gong, G., Waris, G., Tanveer, R., and Siddiqui, A. (2001) Human hepatitis C virus NS5A protein alters intracellular calcium levels, induces oxidative stress, and activates STAT-3 and NF-kappa B, *Proc. Natl. Acad. Sci. U.S.A. 98*, 9599−9604.
12. Tellinghuisen, T. L., Marcotrigiano, J., Gorbalenya, A. E., and Rice, C. M. (2004) The NS5A protein of hepatitis C virus is a zinc metalloprotein, *J. Biol. Chem. 279*, 48576−48587.
13. Brass, V., Bieck, E., Montserret, R., Wolk, B., Hellings, J. A., Blum, H. E., Penin, F., and Moradpour, D. (2002) An amino-terminal amphipathic alpha-helix mediates membrane association of the hepatitis C virus nonstructural protein 5A, *J. Biol. Chem. 277*, 8130−8139.
14. Penin, F., Dubuisson, J., Rey, F. A., Moradpour, D., and Pawlotsky, J. M. (2004) Structural biology of hepatitis C virus, *Hepatology 39*, 5−19.
15. Tellinghuisen, T. L., Marcotrigiano, J., and Rice, C. M. (2005) Structure of the zinc-binding domain of an essential component of the hepatitis C virus replicase, *Nature 435*, 374−379.
16. Shirota, Y., Luo, H., Qin, W., Kaneko, S., Yamashita, T., Kobayashi, K., and Murakami, S. (2002) Hepatitis C virus (HCV) NS5A binds RNA-dependent RNA polymerase (RdRP) NS5B and modulates RNA-dependent RNA polymerase activity, *J. Biol. Chem. 277*, 11149−11155.
17. Street, A., Macdonald, A., Crowder, K., and Harris, M. (2004) The Hepatitis C virus NS5A protein activates a phosphoinositide 3-kinase-dependent survival signaling cascade, *J. Biol. Chem. 279*, 12232−12241.
18. Street, A., Macdonald, A., McCormick, C., and Harris, M. (2005) Hepatitis C virus NS5A-mediated activation of phosphoinositide 3-kinase results in stabilization of cellular beta-catenin and stimulation of beta-catenin-responsive transcription, *J. Virol. 79*, 5006−5016.
19. Bottomley, M. J., Macias, M. J., Liu, Z., and Sattler, M. (1999) A novel NMR experiment for the sequential assignment of proline residues and proline stretches in $^{13}C/^{15}N$-labeled proteins, *J. Biomol. NMR 13*, 381−385.
20. Johnson, B. A. B. R. A. (1994) NMR View−A Computer-Program for the Visualization and Analysis of NMR Data, *J. Biomol. NMR 4*, 603−614.
21. Farrow, N. A., Muhandiram, R., Singer, A. U., Pascal, S. M., Kay, C. M., Gish, G., Shoelson, S. E., Pawson, T., Forman-Kay, J. D., and Kay, L. E. (1994) Backbone dynamics of a free and

phosphopeptide-complexed Src homology 2 domain studied by ^{15}N NMR relaxation, *Biochemistry 33*, 5984−6003.
22. Vojnic, E., Simon, B., Strahl, B. D., Sattler, M., and Cramer, P. (2006) Structure and carboxyl-terminal domain (CTD) binding of the Set2 SRI domain that couples histone H3 Lys36 methylation to transcription, *J. Biol. Chem. 281*, 13−15.
23. Peti, W., Smith, L. J., Redfield, C., and Schwalbe, H. (2001) Chemical shifts in denatured proteins: resonance assignments for denatured ubiquitin and comparisons with other denatured proteins, *J. Biomol. NMR 19*, 153−165.
24. Wishart, D. S., Bigam, C. G., Holm, A., Hodges, R. S., and Sykes, B. D. (1995) ^{1}H, ^{13}C and ^{15}N random coil NMR chemical shifts of the common amino acids. I. Investigations of nearest-neighbor effects, *J. Biomol. NMR 5*, 67−81.
25. Merutka, G., Dyson, H. J., and Wright, P. E. (1995) 'Random coil' ^{1}H chemical shifts obtained as a function of temperature and trifluoroethanol concentration for the peptide series GGXGG, *J. Biomol. NMR 5*, 14−24.
26. Schwalbe, H., Fiebig, K. M., Buck, M., Jones, J. A., Grimshaw, S. B., Spencer, A., Glaser, S. J., Smith, L. J., and Dobson, C. M. (1997) Structural and dynamical properties of a denatured protein. Heteronuclear 3D NMR experiments and theoretical simulations of lysozyme in 8 M urea, *Biochemistry 36*, 8977−8991.
27. Wishart, D. S., Sykes, B. D., and Richards, F. M. (1991) Relationship between nuclear magnetic resonance chemical shift and protein secondary structure, *J. Mol. Biol. 222*, 311−333.
28. Wishart, D. S., and Case, D. A. (2001) Use of chemical shifts in macromolecular structure determination, *Methods Enzymol. 338*, 3−34.
29. Wishart, D. S., and Nip, A. M. (1998) Protein chemical shift analysis: a practical guide, *Biochem. Cell Biol. 76*, 153−163.
30. Wishart, D. S., and Sykes, B. D. (1994) Chemical shifts as a tool for structure determination, *Methods Enzymol. 239*, 363−392.
31. Vuister, G.W., B. A. (1993) Quantitative J correlation: A new approach for measuring homonuclear three-bond J ($H_{NH\alpha}$) coupling constants in ^{15}N-enriched proteins, *J. Am. Chem. Soc. 115*, 7772−7777.
32. Marion, D., Driscoll, P. C., Kay, L. E., Wingfield, P. T., Bax, A., Gronenborn, A. M., and Clore, G. M. (1989) Overcoming the overlap problem in the assignment of ^{1}H NMR spectra of larger proteins by use of three-dimensional heteronuclear ^{1}H-^{15}N Hartmann-Hahn-multiple quantum coherence and nuclear Overhauser-multiple quantum coherence spectroscopy: application to interleukin 1 beta, *Biochemistry 28*, 6150−6156.
33. Hu, Y., Macinnis, J. M., Cherayil, B. J., Fleming, G. R., Freed, K. F., and and Perico, A. (1990) Polypeptide dynamics: experimental tests of an optimized Rouse-Zimm type model, *J. Chem. Phys. 93*, 822−836.
34. Ulrich, D. L., Kojetin, D., Bassler, B. L., Cavanagh, J., and Loria, J. P. (2005) Solution structure and dynamics of LuxU from Vibrio harveyi, a phosphotransferase protein involved in bacterial quorum sensing, *J. Mol. Biol. 347*, 297−307.
35. Thormann, T., Soroka, V., Nielbo, S., Berezin, V., Bock, E., and Poulsen, F. M. (2004) Backbone dynamics of the first, second, and third immunoglobulin modules of the neural cell adhesion molecule (NCAM), *Biochemistry 43*, 10364−10369.
36. Bhavesh, N. S., Sinha, R., Mohan, P. M., and Hosur, R. V. (2003) NMR elucidation of early folding hierarchy in HIV-1 protease, *J. Biol. Chem. 278*, 19980−19985.
37. Dobson, C. M. (1992) Unfolded proteins, compact states and molten globules, *Curr. Opin. Struct. Biol. 2*, 6−12.
38. Adler, A. J., Greenfield, N. J., and Fasman, G. D. (1973) Circular dichroism and optical rotatory dispersion of proteins and polypeptides, *Methods Enzymol. 27*, 675−735.
39. Wang, Y., and Jardetzky, O. (2002) Probability-based protein secondary structure identification using combined NMR chemical-shift data, *Protein Sci. 11*, 852−861.
40. Wootton, J. C. (1994) Non-globular domains in protein sequences: automated segmentation using complexity measures, *Comput. Chem. 18*, 269−285.
41. Tompa, P. (2002) Intrinsically unstructured proteins, *Trends Biochem. Sci. 27*, 527−533.
42. Dyson, H. J., and Wright, P. E. (2002) Coupling of folding and binding for unstructured proteins, *Curr. Opin. Struct. Biol. 12*, 54−60.
43. Tanimoto, A., Ide, Y., Arima, N., Sasaguri, Y., and Padmanabhan, R. (1997) The amino terminal deletion mutants of hepatitis C virus nonstructural protein NS5A function as transcriptional activators in yeast, *Biochem. Biophys. Res. Commun. 236*, 360−364.
44. Uversky, V. N. (2002) What does it mean to be natively unfolded?, *Eur. J. Biochem. 269*, 2−12.
45. Gunasekaran, K., Tsai, C. J., Kumar, S., Zanuy, D., and Nussinov, R. (2003) Extended disordered proteins: targeting function with less scaffold, *Trends Biochem. Sci. 28*, 81−85.
46. Wright, P. E., and Dyson, H. J. (1999) Intrinsically unstructured proteins: re-assessing the protein structure-function paradigm, *J. Mol. Biol. 293*, 321−331.
47. Spolar, R. S., and Record, M. T., Jr. (1994) Coupling of local folding to site-specific binding of proteins to DNA, *Science 263*, 777−784.
48. Donaldson, L., and Capone, J. P. (1992) Purification and characterization of the carboxyl-terminal transactivation domain of Vmw65 from herpes simplex virus type 1, *J. Biol. Chem. 267*, 1411−1414.
49. Kussie, P. H., Gorina, S., Marechal, V., Elenbaas, B., Moreau, J., Levine, A. J., and Pavletich, N. P. (1996) Structure of the MDM2 oncoprotein bound to the p53 tumor suppressor transactivation domain, *Science 274*, 948−953.
50. Uesugi, M., Nyanguile, O., Lu, H., Levine, A. J., and Verdine, G. L. (1997) Induced alpha helix in the VP16 activation domain upon binding to a human TAF, *Science 277*, 1310−1313.
51. Nakayama, K. I., Hatakeyama, S., and Nakayama, K. (2001) Regulation of the cell cycle at the G1-S transition by proteolysis of cyclin E and p27Kip1, *Biochem. Biophys. Res. Commun. 282*, 853−860.
52. Llinas, M., and Klein, M. P. (1975) Charge relay at the peptide bond.Aproton magnetic resonance study of solvation effects on the amide electron density distribution, *J. Am. Chem. Soc. 97*, 4731−4737.
53. Nelson, J. W., and Kallenbach, N. R. (1986) Stabilization of the ribonuclease S-peptide alpha-helix by trifluoroethanol, *Proteins 1*, 211−217.
54. Sonnichsen, F. D., Van Eyk, J. E., Hodges, R. S., and Sykes, B. D. (1992) Effect of trifluoroethanol on protein secondary structure: an NMR and CD study using a synthetic actin peptide, *Biochemistry 31*, 8790−8798.
55. Shiraki, K., Nishikawa, K., and Goto, Y. (1995) Trifluoroethanol-induced stabilization of the alpha-helical structure of beta-lactoglobulin: implication for non-hierarchical protein folding, *J. Mol. Biol. 245*, 180−194.
56. Fink, A. L. (2005) Natively unfolded proteins, *Curr. Opin. Struct. Biol. 15*, 35−41.
57. Uversky, V. N. (2002) Natively unfolded proteins: a point where biology waits for physics, *Protein Sci. 11*, 739−756.
58. Liang, Y., Kang, C. B., and Yoon, H. S. (2006) Molecular and structural characterization of the domain 2 of hepatitis C virus non-structural protein 5A, *Mol. Cells 22*, 13−20.
59. Brems, D. N., Plaisted, S. M., Kauffman, E. W., and Havel, H. A. (1986) Characterization of an associated equilibrium folding intermediate of bovine growth hormone, *Biochemistry 25*, 6539−6543.
60. Cleland, J. L., and Wang, D. I. (1990) Refolding and aggregation of bovine carbonic anhydrase B: quasi-elastic light scattering analysis, *Biochemistry 29*, 11072−11078.
61. Yeh, S. R., and Rousseau, D. L. (1998) Folding intermediates in cytochrome c, *Nat. Struct. Biol. 5*, 222−228.
62. Garbuzynskiy, S. O., Lobanov, M. Y., and Galzitskaya, O. V. (2004) To be folded or to be unfolded?, *Protein Sci. 13*, 2871−2877.
63. Wishart, D. S., and Sykes, B. D. (1994) The ^{13}C chemical-shift index: a simple method for the identification of protein secondary structure using ^{13}C chemical-shift data, *J. Biomol. NMR 4*, 171−180.

BI700776E